Hindawi
Shock and Vibration
Volume 2019, Article ID 4281958, 10 pages
https://doi.org/10.1155/2019/4281958

Research Article

Design and Vibration Isolation Performance of Truss-Type CFRP Raft Frame

Xianglong Wen,[1,2] **Wenhu Li**,[1] **Yuan Fang**,[1] **Chunsheng Song**,[1,3] **and Jinguang Zhang**[1]

[1]*School of Mechanical and Electronic Engineering, Wuhan University of Technology, Wuhan, China*
[2]*Hubei Provincial Engineering Technology Research Center for Magnetic Suspension, Wuhan, China*
[3]*Institute of Advanced Material Manufacturing Equipment and Technology, Wuhan University of Technology, Wuhan, China*

Correspondence should be addressed to Jinguang Zhang; jgzhang@whut.edu.cn

Received 27 November 2018; Accepted 12 February 2019; Published 1 April 2019

Academic Editor: Chengzhi Shi

Traditional raft frame is single in the form of materials and structures. To give full play to its vibration isolation performance, a truss-type CFRP (carbon fiber-reinforced plastics) raft frame was designed and prepared. Based on the composite material mechanics and damping strain energy model, a method combining the finite element simulation and experiment was used to calculate the damping of the designed CFRP truss structure. The modal harmonic response analysis of CFRP truss structure was carried out by virtue of the ABAQUS finite element software to explore the influence of structure parameters on the vibration transmission characteristics of CFRP truss structure and provide reference for the design of a truss-type CFRP raft frame. The truss-type CFRP floating raft vibration isolation platform was established. Given different excitation sources, the truss-type CFRP raft frame designed in this paper was demonstrated to have good vibration isolation effect in most frequency bands by analyzing the acceleration-vibration level differences.

1. Introduction

The floating raft structure has outstanding shock resistance and vibration isolation performance, and it has been widely applied on warships to improve the stealth property. The truss-type floating raft has superior vibration isolation effect because of its unique periodic structure and complex internal energy transmission mechanism [1]. Scholars have carried out a lot of researches to improve the vibration isolation performance of the floating raft frame to study the vibration isolation performance of the raft frame structure by changing the geometric size and number of the subelements of raft frame structure [2–6], to design the new form of the raft frame structure to reduce vibration [7–9], and to study the damping of the raft frame structure hoping to obtain good vibration isolation performance [10–15]. Compared with traditional metal materials, carbon fiber-reinforced composites have such advantages as large specific strength, high specific modulus, high damping, and strong designability [13, 16–18]. Currently, the structure forms of CFRP applied to vibration isolation are mostly of the truss-type structure, including satellite, spaceship, and other aerospace structures [9, 19–21].

With the analysis of research status at home and abroad, it is easy to find that the introduction of truss-type raft frame has ushered in a new development direction to the vibration isolation technology of floating raft. However, few studies are concerned with the influence rules of the structure and stacking parameters of composite truss-type raft frame on its vibration isolation performance.

Therefore, a truss-type CFRP raft frame structure was designed in the paper based on the influence of the damping characteristics and structure parameters of the truss structure on the vibration isolation effect in combination with the excellent mechanical, damping properties, and band gap properties of the periodic structure of carbon fiber composite. The damping ratio of CFRP truss structure was calculated using theoretical models, the influence of CFRP

truss structure parameters on the vibration isolation performance of raft frame was analyzed with the finite element simulation method, and the vibration isolation test platform of truss-type raft frame was established. With the electromagnetic actuator and vibration motor as excitations, respectively, the experimental study on the vibration transmission performance was carried out to evaluate the vibration isolation effect of the designed truss-type CFRP raft frame by virtue of acceleration-vibration level difference.

2. Simulation

2.1. Numerical Calculation Model of the Damping of Truss-Type CFRP Raft Frame. Under external excitations, the forced vibration equation of the structure is

$$[M]\{\ddot{\delta}\} + [C]\{\dot{\delta}\} + [K]\{\delta\} = \{f(t)\}. \quad (1)$$

In this paper, a finite element method is used to analyze the dynamic response of composite structure, and the specific damping capacity (SDC) is used to represent the damping of composite structure. SDC is defined as the ratio of dissipated energy of the structure ΔU to the maximal strain energy U stored in the structure within one period with the relation between them expressed as

$$\psi = 2\pi\eta = \frac{\Delta U}{U}. \quad (2)$$

The basic method of the strain energy model based on finite element is to conduct modal analysis of the structure using ABAQUS software, extract the stress strain component, and calculate the strain energy of each element. Besides, the damping loss factor of carbon fiber composite has anisotropic characteristic, so in solving the element strain energy, it must be decomposed into the strain energy component corresponding to the stress component in six directions as formula (3); the total strain energy and dissipated energy of the system is the cumulative sum of the strain energy and dissipated energy of all structure elements, and the relation between them is expressed as formula (4).

$$U^k = \sum_{\mathrm{p}}^{N} \sum_{\mathrm{q}}^{6} U^k_{\mathrm{p,q}}, \quad (3)$$

where N is the number of layers for element k and $U^k_{\mathrm{p,q}}$ is the strain energy component corresponding to each stress component at the layer p for element k.

$$\eta = \frac{\sum_{k=1}^{n} \eta_{ij} U^k_{ij}}{\sum_{k=1}^{n} U^k_{ij}}, \quad (i, j = 1, 2, 3), \quad (4)$$

where 1, 2, and 3 represent fiber direction, vertical fiber direction and thickness direction, respectively, and η_{ij} and U^k_{ij} are the loss factor and strain energy component corresponding to the stress component σ_{ij} for the k^{th} element in the composite with the following calculation formula:

$$U^k_{ij} = \frac{1}{2} \int \sigma^k_{ij} \varepsilon^k_{ij} dV^k. \quad (5)$$

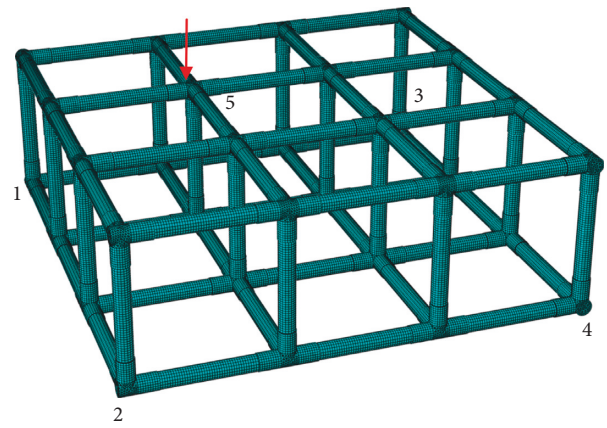

Figure 1: Finite element model and layout of measure points of truss.

2.2. Simulation Calculation of the Damping of CFRP Truss. The overall dimension of the CFRP truss structure under study is 813 mm × 813 mm × 291 mm, composed of the combination of 3 × 3 hexahedral truss frame subelements (as shown in Figure 1). The outer diameter of the truss circular tube is all 28 mm, the wall thickness 2 mm, and the length 231 mm; the material is T700/YPH-308, the stacking scheme is $(\pm 45)_5$, and the stacking layers is 10. Considering the experimental cost and the complexity of molding process, the split mounting truss structure of metal multiple-pass joints (wall thickness 1 mm) connected with CFRP circular tubes is used. When the CFRP periodic truss bears dynamic load, its bar elements show certain periodicity and regularity. To simplify the calculation of damping analysis of the CFRP truss structure, the subelements of CFRP truss structure are selected for analysis within the allowed margin of error.

The damping loss factor of metal materials is usually a constant value, generally 0.01%–0.06%. The material of the joints used is plain carbon steel, and the loss factor is taken 0.03%. The calculation of the damping loss factor of the composite circular tube requires the extraction of stress and strain components in the six directions of all the elements at each layer of all the circular tubes in each order modal of CFRP truss structure. Figure 2 shows the strain cloud diagram of CFRP truss circular tubes under the vibration in the first-order modal.

It is seen from Figure 2 that, in the case of vibration in the first-order modal of CFRP truss structure elements, the strain components of most elements in the thickness direction are 1-2 orders of magnitude smaller than the strain components in axial and circumferential directions, and the strain distribution in the second- and third-order modal also conforms to this rule. Therefore, in calculating the damping ratio of CFRP truss, the in-plane strain energy is the only concern and the out-of-plane strain energy is ignored.

According to the numerical calculation model of composite damping in conjunction with the modal analysis results, the MATLAB program is written to calculate the damping loss factors of 12 CFRP circular tubes, and the damping ratio of each circular tube is calculated with the

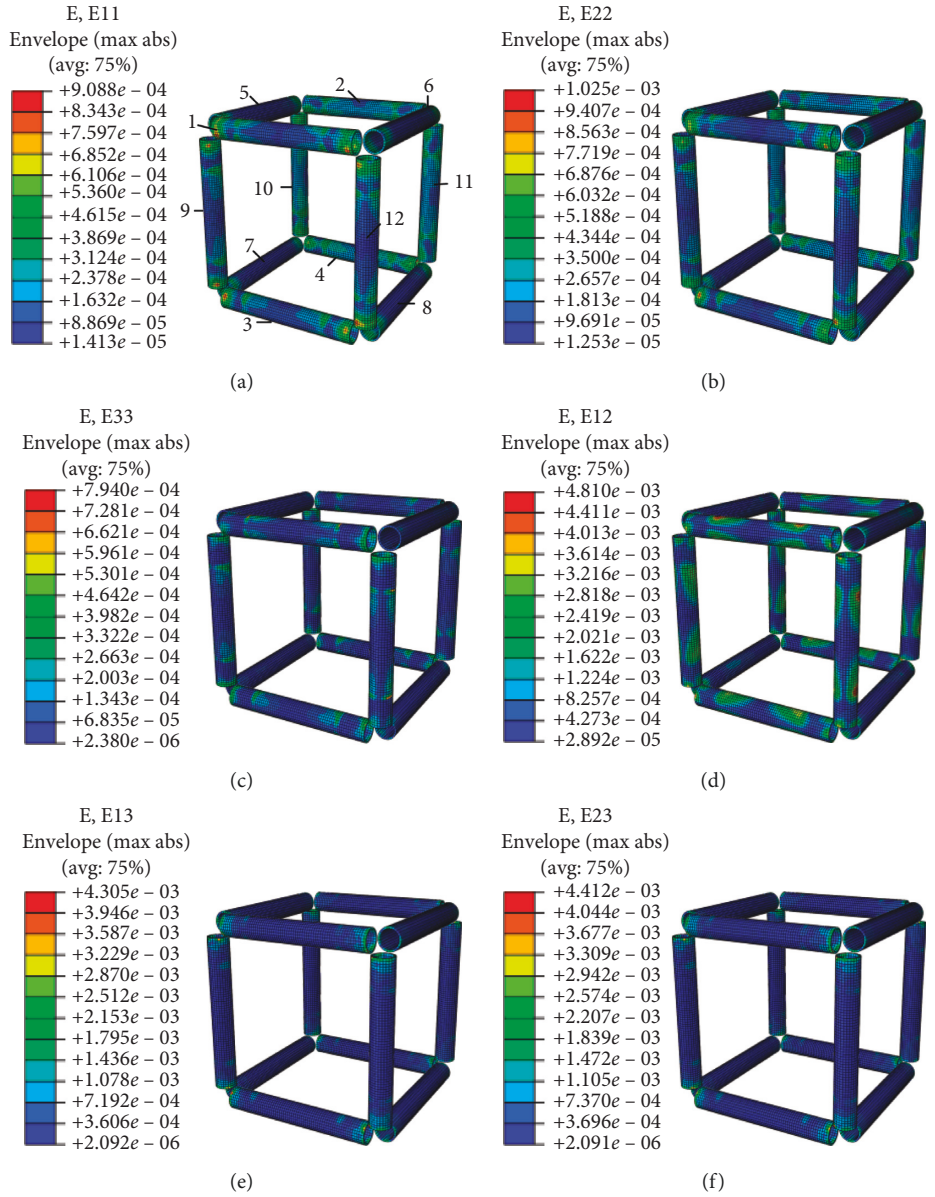

Figure 2: Strain cloud diagram of CFRP truss elements. Strain component in directions (a) 11, (b) 22, (c) 33, (d) 12, (e) 13, and (f) 23.

damping loss factors via formula (6), where the numbers 1–4 refer to the circular tubes in the x direction, 5–8 are the circular tubes in the y direction, and 9–12 are the circular tubes in the z direction; the results are shown in Table 1.

$$\xi = \frac{\eta}{\sqrt{4+\eta^2}}. \tag{6}$$

The modal vibration shape diagrams for the first three orders of CFRP truss subelements are extracted as shown in Figure 3.

It is seen from Figure 3 that the modal shapes of the first three orders of CFRP truss subelements are all bending modals for different circular tubes. By combining the damping ratio of the first three orders of each rod piece in Table 1, it is found that the first order is mainly shown as the bending modal of circular tubes in the x and y directions, and the damping ratios of the circular tubes in such directions are greater than that of circular tubes in the z direction. The second order mainly shows the bending modal of circular tubes the in x and z directions. The damping ratios of circular tubes in these directions are obviously greater than those of the tubes the in y direction. Similarly, a similar conclusion is drawn in the third-order modal, where the damping ratios of the tubes in y and z are significantly greater than those of the tubes in the x direction, and the same circular tube is in the same vibration mode, even if the vibration order is different, the damping ratio is similar. To probe into the overall damping of CFRP truss structure, the dissipated energy and strain energy of all elements of CFRP truss containing metal joints are calculated for summation,

Table 1: Damping ratios of the first three orders for CFRP circular tubes.

Numbering	First-order damping ratio (%)	Second-order damping ratio (%)	Third-order damping ratio (%)
1	3.06	3.03	2.52
2	2.98	3.00	2.32
3	3.07	3.01	2.29
4	3.01	3.08	2.43
5	2.93	2.23	3.07
6	3.11	2.38	2.98
7	3.09	2.25	3.02
8	2.97	2.30	3.08
9	1.98	3.15	2.92
10	2.06	2.93	3.14
11	2.04	2.83	3.12
12	2.04	3.13	2.91

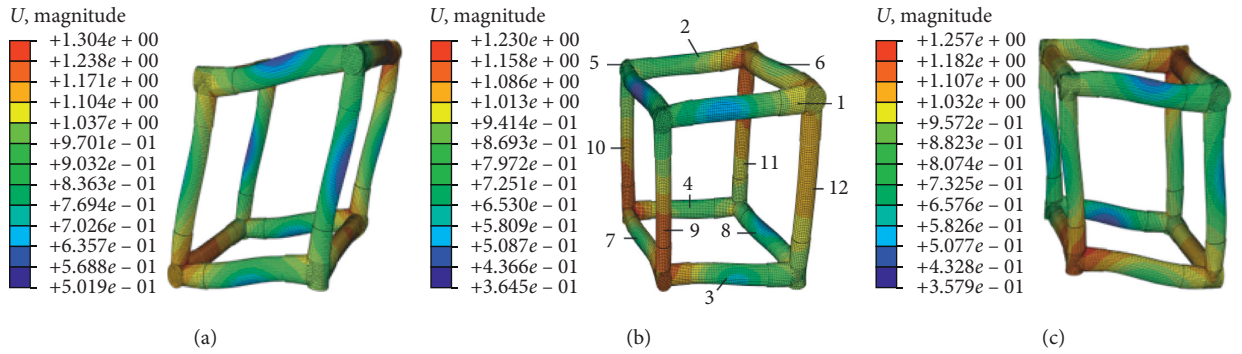

Figure 3: Modal shapes of the (a) first order, (b) second order, and (c) third order of CFRP truss subelements.

and the damping loss factors of CFRP truss structure containing metal joints in the first three order modals are calculated according to formulas (4), (5), and (7):

$$\eta = \frac{\eta_m U_m + \Delta U_c}{U_m + U_c}, \tag{7}$$

where η_m is the damping loss factor of metal materials, U_m is the sum of modal strain energy for eight joints, and ΔU_c and U_c are the sum of strain dissipated energy and modal strain energy for 12 composite circular tubes, respectively. The stress strain values of all elements for CFRP truss subelements are extracted, and the first three orders of damping ratios of the entire truss structure are obtained through MATLAB programming calculation, namely, 1.85%, 1.91%, and 1.94%. The results show that the modal order has little influence on the structure damping.

2.3. Influence of Structure Parameters on the Vibration Performance of CFRP Truss. The design parameters of truss structure include the wall thickness of CFRP circular tubes, the number of periodic elements, and wall thickness and material of joints. The influence of circular tube wall thickness and joint wall thickness on the vibration performance of the truss structure will be studied next to provide the basis for the design of truss-type CFRP raft frame structure.

2.3.1. Tube Wall Thickness of CFRP Truss. The study object in this section is the CFRP truss aforementioned. When other sizes remain unchanged, the wall thickness of the truss rod pieces takes 1 mm, 2 mm, and 3 mm, respectively, for the harmonic response analysis. The finite element model and the location of measure points are as shown in Figure 1.

The 1N normal excitation is applied at the central node of the No. 5 joint in the upper truss, and the vibration displacement responses at the central nodes of four angles on the undersurface of the truss are calculated. For convenience of comparison and computing, the vibration displacement value is expressed in the decibel value according to the following formula:

$$L = 20 \log_{10}\left(\frac{x_i}{\text{ref}}\right) \quad \text{(dB)}, \tag{8}$$

where x_i represents the displacement value of the vibration and ref represents the reference displacement value, and the displacement reference value is 10^{-12} m, according to the GB 50894-2013. The results of harmonic response analysis are shown in Figure 4.

Figure 4 shows the influence of the rod piece wall thickness on the vibration transmission of CFRP truss. Firstly, the vibration amplitude in resonance decreases with the increase of the tube wall thickness, and it is more apparent in the high-frequency section. Secondly, the increase of the tube wall thickness narrows down the truss bandstop

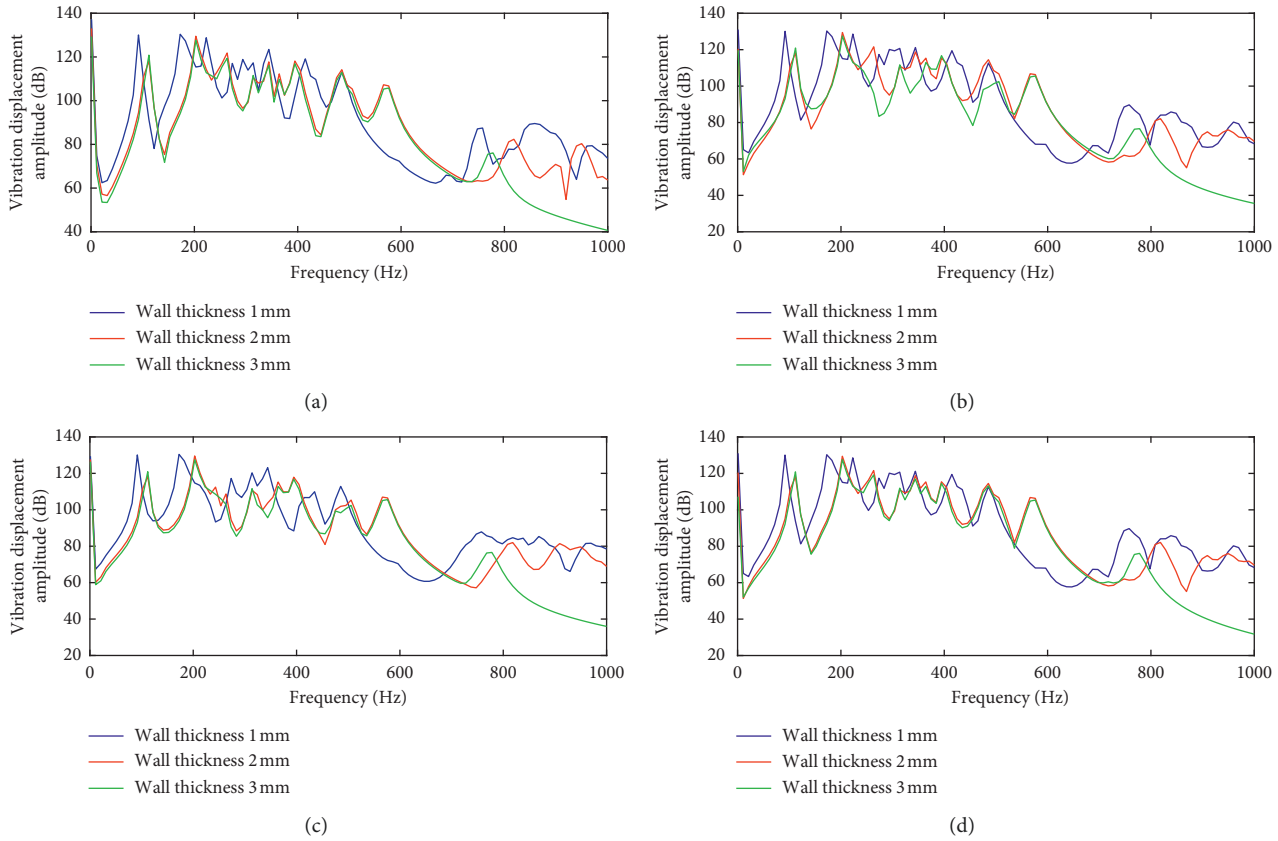

Figure 4: Harmonic response curves at different wall thicknesses at measuring points (a) 1, (b) 2, (c) 3, and (d) 4.

frequency band, which is mainly due to the increase of bending stiffness of the rod piece and the wave effect suppression of truss structure. This indicates that the band gap effect of the truss should be taken into account in designing the CFRP truss structure parameters, and the resonance frequency bands should be avoided by adjusting the structure parameters.

2.3.2. Joint Wall Thickness of CFRP Truss. Trusses with the joint wall thickness of 1 mm, 2 mm, and 3 mm are selected for simulation analysis to study the influence of joint wall thickness on the vibration performance of the entire truss. The exertion of excitation and location of measure points are consistent with Figure 1, and the vibration response of each measure point is shown in Figure 5.

Figure 5 shows the influence of joint wall thickness on the vibration response of CFRP truss. Firstly, the resonance peaks in each order of the truss are subjected to the combined action of the truss mass and stiffness. Secondly, the increase of joint wall thickness widens the bandstop frequency band of CFRP truss.

3. Experimental

3.1. Modal Experiment of CFRP Truss. A free modal test of the designed CFRP truss is conducted using the hammer excitation method to verify the validity of damping computation simulation of the CFRP truss. The test piece is suspended on the support with a good elastic rubber rope to simulate the free support mode, and the acceleration sensors are separately arranged at the central nodes of the six joints on the middle surface of the upper truss as shown in Figure 6.

In the experiment, excitation is exerted on the six measure points corresponding to the acceleration sensors on the back of the truss for three times for the purpose of analysis and solution of the frequency response functions, and the frequency response curves measured by each sensor are input into Modal Genius software for processing and fitting to obtain the modal damping ratios of the first three orders for the CFRP truss. The test and simulation results are shown in Table 2.

By comparing the modal damping ratios of the first three orders of CFRP truss, it is found that the damping ratios obtained from the aforementioned models are consistent with those of the first three orders measured in the experiment within the allowed margin of error, which tentatively verifies the accuracy of the damping numerical calculation model of CFRP truss.

3.2. Vibration Isolation Test of Truss-Type Floating Raft

3.2.1. Experimental Setup. The truss-type CFRP floating raft isolation test platform constructed in this paper is mainly composed of a vibration motor, electromagnetic actuator, motor support plate, upper and lower mounting plates,

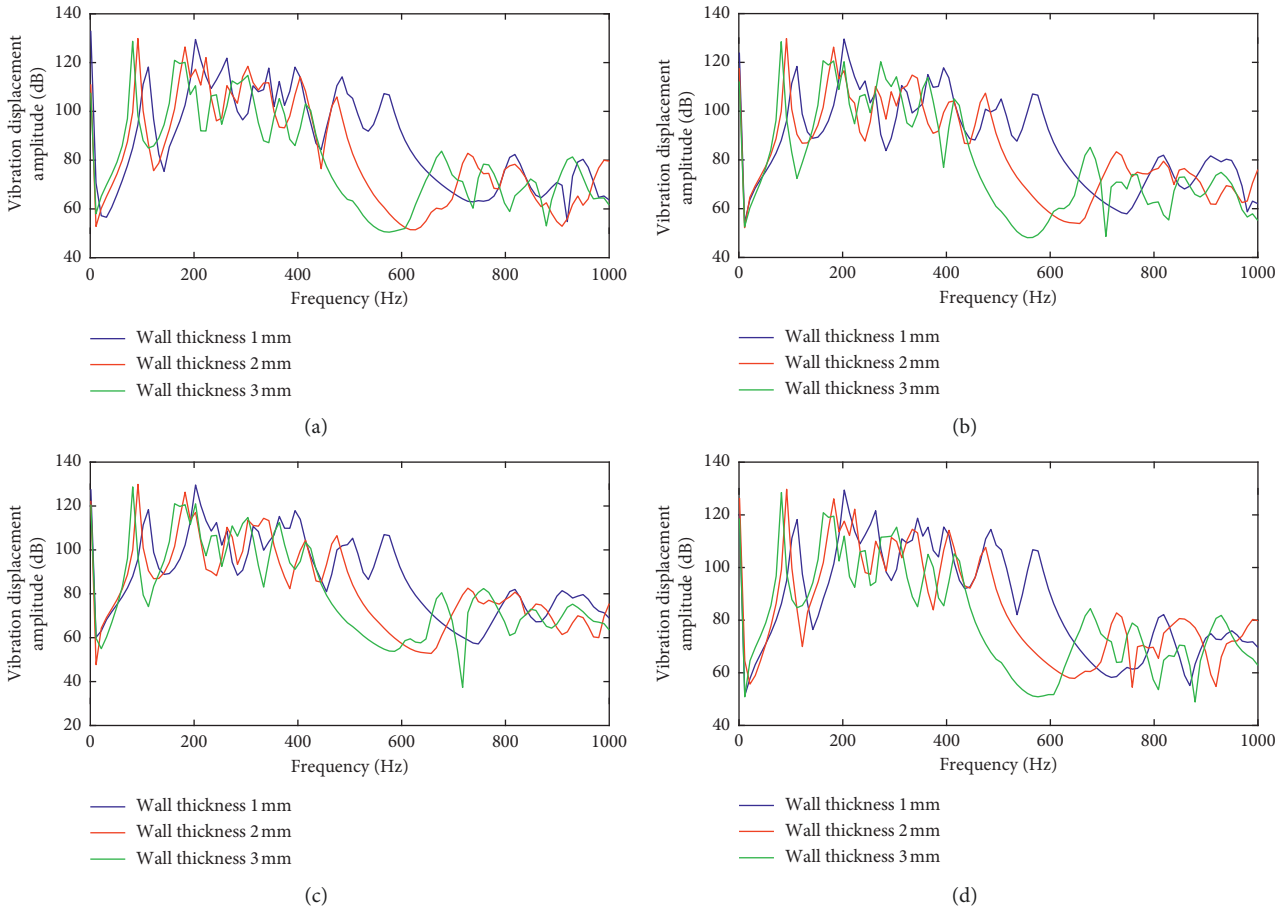

Figure 5: Harmonic response curves at different joint wall thickness at measuring points (a) 1, (b) 2, (c) 3, and (d) 4.

Figure 6: Modal experiment of CFRP truss.

rubber vibration isolator, CFRP truss-type raft frame, and air spring and foundation support as shown in Figure 7.

The mounting plate is made of carbon fiber composite and fixed via mechanical connection with the CFRP truss. The vibration motor set is rigidly fixed connected with the motor support plate through bolts, and the motor speed is adjusted with a frequency converter to obtain sinusoidal signals of different specific frequencies. The model of the electromagnetic actuator is jzk-50. The ejector rod is connected with the lower mounting plate with the nuts to generate linear swept-frequency signals. The motor support plate is elastically connected with the upper mounting plate of the raft frame through four rubber vibration isolators. The air spring model is 086060h-1, and it is pressurized by the air compressor. The foundation support is connected to the lower mounting plate of the raft frame through four pressure adjustable air springs and is rigidly fixed onto the T-table through bolts.

3.2.2. Experimental Study on the Vibration Isolation Performance of CFRP Truss Excited by Swept-Frequency Signals. Seven acceleration sensors are selected for the vibration isolation performance test under the excitation of swept-frequency signals, and their installation positions are shown in Figure 8. No. 1 and No. 2 acceleration sensors measure the acceleration at the vibration motor. No. 3 and No. 4 acceleration sensors measure the acceleration at the upper end of the truss; No. 5 and No. 6 acceleration sensors measure the acceleration at the lower end of the truss. No. 7 acceleration sensor measures the acceleration at the vibration input end. To guarantee the reliability of the experimental

Table 2: Experimental and simulation calculation errors of damping.

Order	Damping ratio (%)		
	Simulation	Experiment	Error (%)
1	1.85	1.98	6.6
2	1.91	1.75	8.3
3	1.94	1.80	7.2

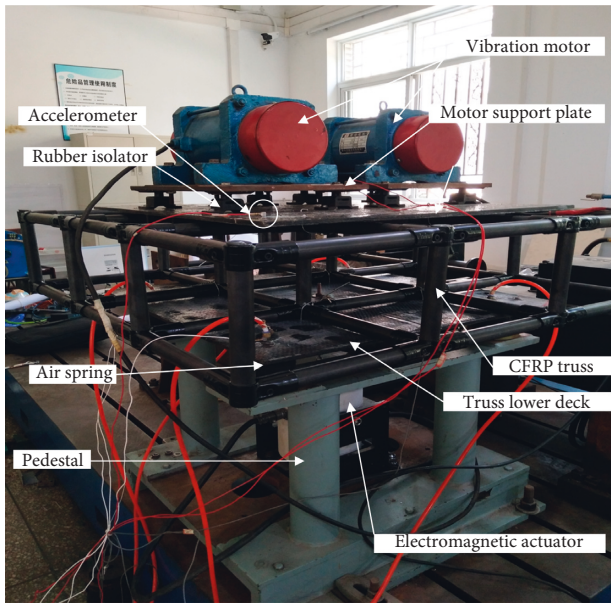

Figure 7: Vibration isolation test platform of the CFRP truss-type floating raft.

measurements, the seven acceleration sensors selected need to be calibrated.

When the vibration transmission characteristics of the truss-type CFRP floating raft system under the excitation of swept-frequency signals are studied, the electromagnetic actuator serves at the vibration input end, and the measured data of seven acceleration sensors are input into MATLAB software; the acceleration-vibration level differences of No. 7 measure point and No. 1–6 measure points are calculated, which are the acceleration-vibration level differences of the vibration input end and each layer of truss-type CFRP floating raft vibration isolation system as shown in Figure 9.

In Figure 9, the vertical coordinates are the acceleration-vibration level differences of No. 7 measure point and No. 1–6 measure points, respectively. The larger the value, the better the vibration isolation effect. From Figure 9, it is observed that the acceleration-vibration level differences of No. 1, No. 2, and No. 7 sensors are the largest, and the average value is above 20 dB. It shows that the truss-type CFRP raft frame designed in this paper can attenuate the bottom-up vibration transmission significantly. It is indicated from Figure 9 that the vibration isolation effect of the designed truss-type raft frame is not very ideal in the low-frequency section, which also conforms to the universal laws of passive vibration isolation.

3.2.3. Vibration Isolation Test of Truss Excited by Simple Harmonic Signals of a Specific Frequency. To make the excitation source more in line with the actual working conditions, the vibration motor set is used as the vibration source in this section for the test. This time, the vibration motor serves as the input end of vibration, and No. 1 and No. 2 acceleration sensors measure the acceleration at the input end of vibration. No. 3 and No. 4 acceleration sensors measure the acceleration at the upper end of the CFRP truss; Nos. 5, 6, and 7 sensors measure the vibration acceleration at the lower end of the truss. The converter frequency is set to 20 Hz and 25 Hz, respectively, and FFT is conducted on the measured data by using No. 3 and No. 6 sensors at the set frequencies as shown in Figures 10 and 11.

Since the vibration input is simple harmonic signals at 20 Hz and 25 Hz, we only need to focus on the acceleration response values at 20 Hz and 25 Hz in the frequency domain graph. From Figures 10 and 11 the acceleration vibration amplitudes of No. 3 and No. 6 sensors at 20 Hz and 25 Hz are obtained directly and the acceleration-vibration level differences are calculated as shown in Table 3.

It is learned from Table 3 that, under the excitation of two specific frequencies, the truss-type CFRP raft frame shows good vibration suppression effect, and the isolation effect is superior in relatively high frequency bands, which also conforms to the experimental results under swept frequency of electromagnetic excitation.

4. Conclusions

A CFRP truss-type floating raft structure was designed in this paper, and a combined method of simulation and experiment was used to study its inherent properties and dynamic characteristics. The strain energy model of the CFRP truss was set up, and the damping ratio of CFRP truss structure was calculated with the explanation of damping characteristics from the perspective of energy dissipation mechanism given. The influence rule of structure parameters of CFRP truss-type raft frame on its vibration transmission characteristics was studied. A CFRP truss-type floating raft vibration isolation test platform was constructed, and the vibration isolation test of CFRP truss-type floating raft was performed using the electromagnetic actuator and vibration motor as the vibration sources with the acceleration-vibration level differences of the raft frame upper surface and the foundation support as evaluation indexes. Based on the above work, the main conclusions drawn from this paper are as follows:

(1) It is known from Tables 1 and 2 that the damping of truss is related to its vibration mode but unrelated to the order, and the damping values calculated within the allowed margin of error are almost the same as the measured values, which indicates that the damping numerical calculation model of constructed is correct.

(2) Through the analysis of Figures 4 and 5, it is observed that the thicker the CFRP circular tube wall, the smaller the vibration amplitude of the truss and the

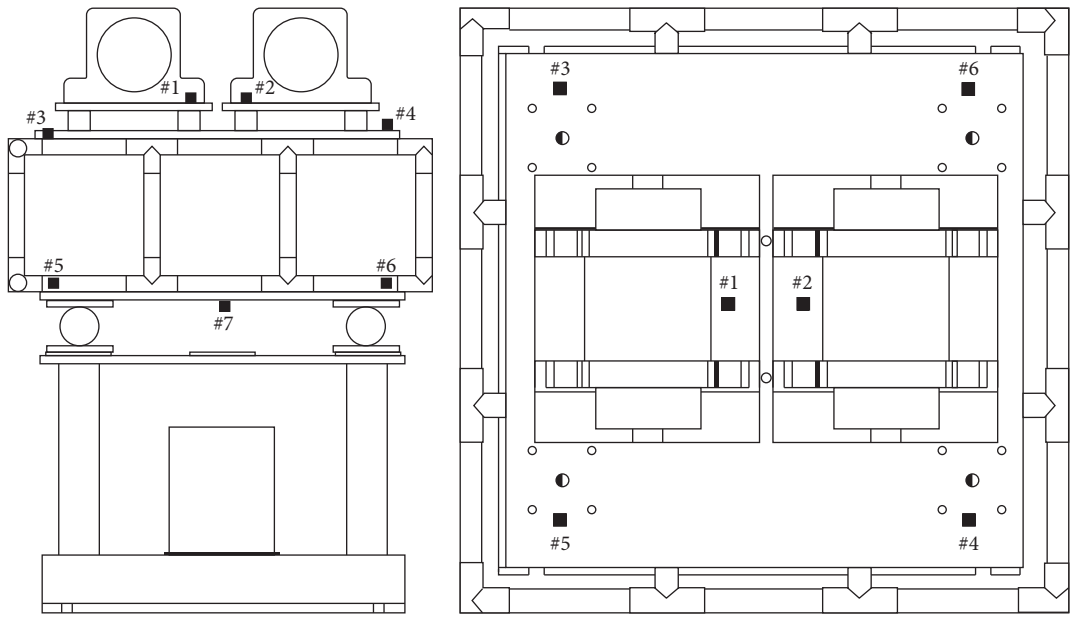

Figure 8: Installation positions of the acceleration sensors: (a) elevation and (b) horizontal layout.

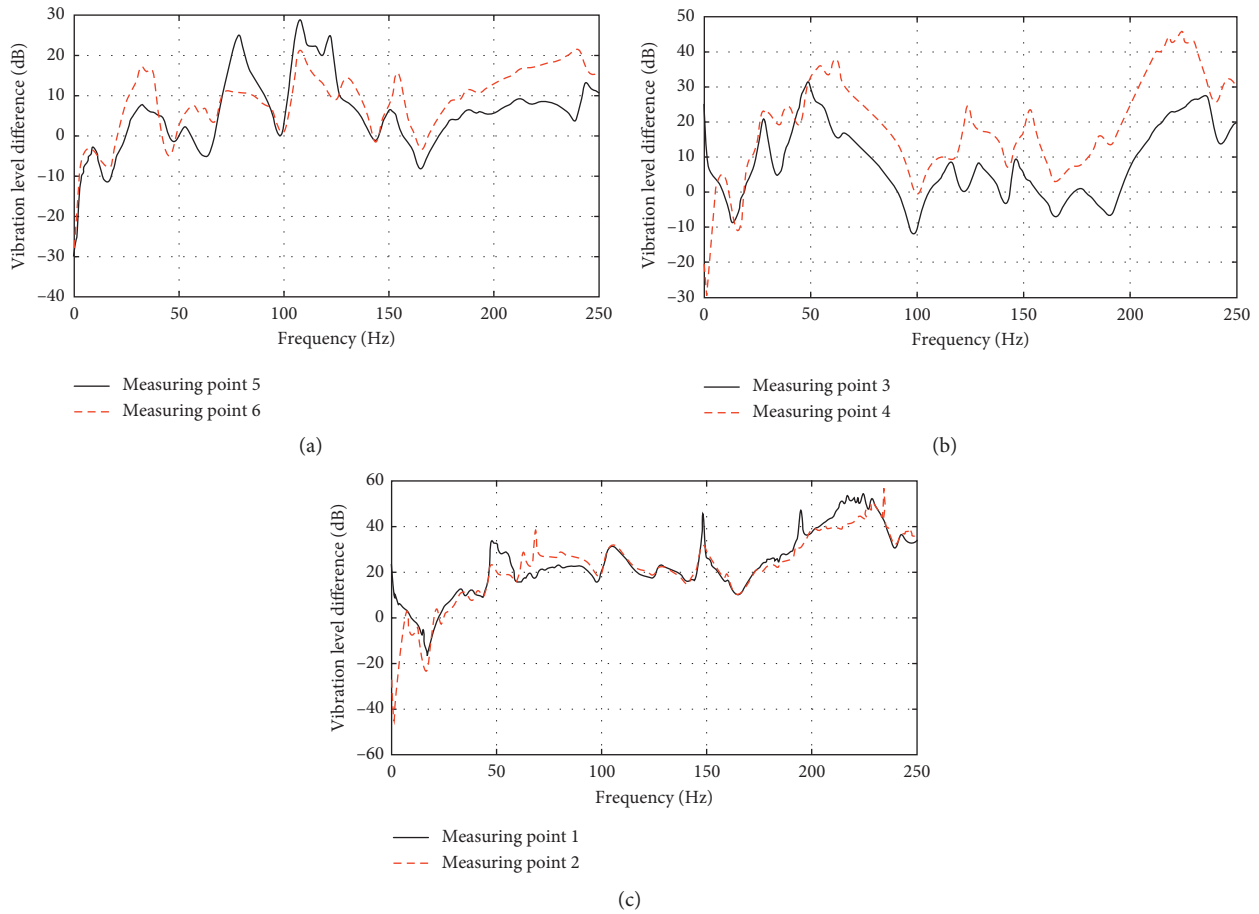

Figure 9: Acceleration-vibration level differences. Measuring points: (a) 5 and 6, (b) 3 and 4, and (c) 1 and 2.

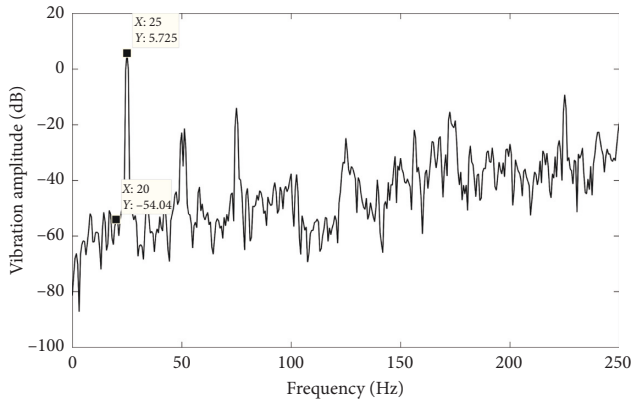

Figure 10: Spectrum at the vibration input end of the truss frame.

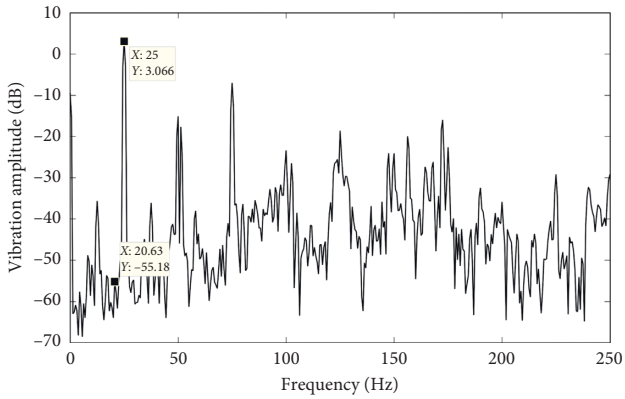

Figure 11: Spectrum at the vibration output end of the truss frame.

Table 3: Acceleration-vibration level difference of raft frame at specific frequencies.

Dominant frequency	Vibration input end of the raft frame	Vibration output end of the raft frame	Acceleration-vibration level difference
20 Hz	−54.04 dB	−55.18 dB	1.14 dB
25 Hz	5.73 dB	3.07 dB	2.66 dB

narrower the bandstop frequency band. The larger the joint thickness, the wider the bandstop frequency band of the truss, which provides reference for the design of the truss structure.

(3) As analyzed from Figure 9, when the electromagnetic actuator serves as the excitation source, the designed CFRP truss-type floating raft structure has good vibration isolation effect in all frequency bands of 0–250 Hz except for the vibration amplification signs shown in the low-frequency section below 5 Hz. It is revealed from Table 3 that the designed truss-type CFRP raft frame has good damping effect at all particular vibration frequencies, which also verifies the reasonableness of the designed truss-type CFRP floating raft structure.

Data Availability

The data used to support the findings of this study are available from the corresponding author upon request.

Conflicts of Interest

The authors declare that they have no conflicts of interest.

Acknowledgments

This research was supported by the National Natural Science Foundation of China (nos. 51879209 and 51775400).

References

[1] S. Ju, R. A. Shenoi, D. Jiang, and A. J. Sobey, "Multi-parameter optimization of lightweight composite triangular truss structure based on response surface methodology," *Composite Structures*, vol. 97, no. 2, pp. 107–116, 2013.

[2] I. V. Andrianov, J. Awrejcewicz, B. Markert, and G. A. Starushenko, "Analytical homogenization for dynamic analysis of composite membranes with circular inclusions in hexagonal lattice structures," *International Journal of Structural Stability & Dynamics*, vol. 17, no. 5, article 1740015, 2017.

[3] T. Delpero, S. Schoenwald, A. Zemp, and A. Bergamini, "Structural engineering of three-dimensional phononic crystals," *Journal of Sound and Vibration*, vol. 363, no. 2, pp. 156–165, 2016.

[4] K. Koohestani and A. Kaveh, "Efficient buckling and free vibration analysis of cyclically repeated space truss structures," *Finite Elements in Analysis and Design*, vol. 46, no. 10, pp. 943–948, 2010.

[5] C.-Y. Zhu, Y.-H. Zhao, S. Gao, and X.-F. Li, "Mechanical behavior of concrete filled glass fiber reinforced polymer-steel tube under cyclic loading," *Journal of Zhejiang University Science A*, vol. 14, no. 11, pp. 778–788, 2013.

[6] A. Salehian and T. Seigler, "Dynamic effects of embedded macro-fiber composite actuators on ultra-light flexible structures of repeated pattern-a homogenization approach," *Shock & Vibration*, vol. 19, no. 1, pp. 81–100, 2015.

[7] J. B. Berger, H. N. G. Wadley, and R. M. McMeeking, "Mechanical metamaterials at the theoretical limit of isotropic elastic stiffness," *Nature*, vol. 543, no. 7646, pp. 533–537, 2017.

[8] Z. Feng, B. Zhenguo, L. Xiaobin, and Y. Mengsa, "Design and experiment of a cradle truss type floating raft system," *Journal of the Acoustical Society of America*, vol. 131, no. 4, p. 3307, 2012.

[9] J. Schäfer, T. Isenbügel, and T. Gries, "Truss structures made of carbon-fibre-reinforced plastic," *Lightweight Design Worldwide*, vol. 10, no. 1, pp. 36–39, 2017.

[10] A. Ahuja and S. Gupta, "Fuzzy logic controlled semi-active floating raft vibration isolation system," *Universal Journal of Mechanical Engineering*, vol. 2, no. 4, pp. 142–147, 2014.

[11] A. Fereidoon and A. H. Niyari, "Investigation of the nonlinear behaviour of damping of aluminum foam core sandwich composite beams," *Journal of Reinforced Plastics and Composites*, vol. 31, no. 9, pp. 639–653, 2012.

[12] J. Meaud, T. Sain, B. Yeom et al., "Simultaneously high stiffness and damping in nanoengineered microtruss composites," *ACS Nano*, vol. 8, no. 4, pp. 3468–3475, 2014.

[13] J. Yang, J. Xiong, L. Ma, G. Zhang, X. Wang, and L. Wu, "Study on vibration damping of composite sandwich

cylindrical shell with pyramidal truss-like cores," *Composite Structures*, vol. 117, no. 1, pp. 362–372, 2014.

[14] J.-S. Yang, L. Ma, R. Schmidt et al., "Hybrid lightweight composite pyramidal truss sandwich panels with high damping and stiffness efficiency," *Composite Structures*, vol. 148, pp. 85–96, 2016.

[15] M. Altan, M. Bayraktar, and B. Yavuz, "Manufacturing polymer/metal macro-composite structure for vibration damping," *International Journal of Advanced Manufacturing Technology*, vol. 86, no. 5–8, pp. 2119–2126, 2016.

[16] H. A. Deveci and H. S. Artem, "On the estimation and optimization capabilities of the fatigue life prediction models in composite laminates," *Journal of Reinforced Plastics and Composites*, vol. 37, no. 21, pp. 1304–1321, 2018.

[17] J. H. Lee, K. S. Kim, and H. Kim, "Determination of kinetic parameters during the thermal decomposition of epoxy/carbon fiber composite material," *Korean Journal of Chemical Engineering*, vol. 30, no. 4, pp. 955–962, 2013.

[18] Y. Li and D. Xu, "Vibration attenuation of high dimensional quasi-zero stiffness floating raft system," *International Journal of Mechanical Sciences*, vol. 126, pp. 186–195, 2017.

[19] F. Fan, D. Kong, M. Sun, and X. Zhi, "Anti-seismic effect of lattice grid structure with friction pendulum bearings under the earthquake impact of various dimensions," *International Journal of Steel Structures*, vol. 14, no. 4, pp. 777–784, 2014.

[20] A. Mroz, A. Orlowska, and J. Holnicki-Szulc, "Semi-active damping of vibrations. prestress accumulation-release strategy development," *Shock & Vibration*, vol. 17, no. 2, pp. 123–136, 2010.

[21] A. Shanygin, E. Dubovikov, V. Fomin, I. Mareskin, and M. Zichenkov, "Designing pro-composite truss layout for load-bearing aircraft structures," *Fatigue & Fracture of Engineering Materials & Structures*, vol. 40, no. 10, pp. 1612–1623, 2017.